Humanlike representation of social networks in large language models

Jae-Young Son[1,2*], Daniel L. Carstensen[1,3*], & Serra E. Favila[1,2]

[1] Department of Cognitive & Psychological Sciences, Brown University
[2] Robert J. and Nancy D. Carney Institute for Brain Science, Brown University
[3] Current Address: Department of Psychology, University of Pennsylvania
* Equal contribution

Corresponding Authors:
Jae-Young Son (jae@brown.edu) & Serra E. Favila (serra_favila@brown.edu)

ABSTRACT

Although large language models (LLMs) have made great progress in their general reasoning capabilities, reasoning about social relationships has remained a challenge. In contrast, humans are naturally skilled at reasoning about how people are connected to one another, even in large, complex social networks. Recent research in cognitive science suggests that a key component of human social intelligence is the ability to represent social networks using *multistep abstraction*, which integrates knowledge of both direct and indirect social connections, and therefore supports inferences about network members' social proximity to one another. Here, we test whether LLMs represent social networks using similar computational principles. In Study 1, we converted an existing human social navigation task into text and recorded LLM responses to the same problems humans were tasked with solving. LLMs' behaviors closely mirrored those of human participants, and were best-explained by Katz communicability, a model of multistep abstraction that captures how humans represent and navigate social networks. In Study 2, we tested whether these multistep representations persisted in a task where they offered no benefit—and were in fact detrimental to task accuracy—and found that LLMs continued to show a multistep signature even in this context. These findings suggest that multistep abstraction may be a core property of how LLMs represent relational information, closely paralleling accounts of human cognitive maps.

INTRODUCTION

Adaptive social behavior, like predicting where gossip might spread if shared with a particular individual, requires knowledge of how people are connected to one another. Humans are skilled at solving these kinds of social navigation problems, even within large, complex social networks

(Dodds et al., 2003; Momennejad, 2021; Son et al., 2024; Travers & Milgram, 1969; Xia et al., 2025). In contrast, large language models (LLMs) continually struggle to reason appropriately about social relationships (Mineault et al., 2026; Momennejad et al., 2023; Song et al., 2026; Xu et al., 2025), despite significant advances in their overall reasoning and problem-solving abilities. Understanding how LLMs represent social structure is therefore critical for identifying which representational properties are necessary for building AI systems that produce more humanlike social cognition and can reason reliably about human relationships.

Social navigation, like its spatial counterpart, can be understood as a form of graph traversal, in which nodes represent people (or places) and edges represent the relationships (or paths) connecting them. In both domains, LLMs often exhibit poor performance and make systematic errors (Momennejad et al., 2023; Yamada et al., 2023). For example, LLMs often hallucinate edges that do not actually exist, then attempt to traverse nodes through these non-existent connections (Momennejad et al., 2023). While these behaviors provide clear evidence against emergent model-based planning in LLMs, systematic errors are often diagnostic of the capacities and constraints of the systems producing them (Binz & Schulz, 2023; Griffiths, 2020; Lieder & Griffiths, 2020). It is therefore possible that systematic navigation errors can help reveal how a boundedly-rational system generates structured relational representations given the computational resources available to it (Lynn & Bassett, 2020; Momennejad et al., 2017).

Supporting this view in the spatial domain, LLMs make systematic navigation errors based on spatial proximity, which are consistent with structured (though imperfect) representations of latent graph topology (Yamada et al., 2023). A parallel body of work has documented analogous social proximity errors in how humans represent social networks: humans falsely remember friendships between people who are close by in the network but not actually connected (Brands, 2013; Krackhardt, 1987; Smith et al., 2020). More recent work suggests that these errors arise from learning abstracted cognitive maps of social networks (FeldmanHall et al., 2025), which encode knowledge of both direct connections (e.g., friendships), as well as indirect, multistep connections (e.g., friends-of-friends). While multistep abstraction supports social navigation over long distances (Son et al., 2024), it comes at the cost of systematic memory errors, like falsely remembering friendship between individuals who share many mutual friends, or who belong to the same community (Son et al., 2023; Teoh et al., 2026). However, whether multistep representational structure can also explain LLM social navigation behavior remains untested.

If LLMs *do* generate multistep representations, a second question centers around *when* these representations are expressed. Human experiments have shown that people learn multistep cognitive maps even when they are not needed for social navigation, even at the cost of having less accurate memory of specific social relationships (Son et al., 2023). In other words, multistep representations appear so useful for social reasoning, that people are biased to learn abstracted cognitive maps even when they are not strictly necessary. Given that LLMs appear capable of flexibly generating task-appropriate representations as needed (Binz et al., 2025), it is possible that LLMs only generate multistep representations when they are relevant for social navigation. Alternatively, like humans, LLMs might generate multistep representations even when they are task-irrelevant.

Here, we investigate these questions across two studies. In Study 1, we tested whether multistep abstraction can account for LLMs' social navigation behavior. If this is the case, LLM errors should mirror human errors, preferentially inferring connections between individuals who share many mutual contacts or who belong to the same community, rather than hallucinating edges at random. To test this, we converted an existing social navigation task into text prompts, then recorded LLMs' responses to the same problems that humans had previously been tasked with solving. This allowed us to precisely quantify the degree of similarity between human and LLM navigation accuracy, including systematic errors made by both humans and LLMs. Using a computational cognitive modeling approach, we also leveraged fine-grained patterns in LLMs' next-token probability distributions to test whether multistep representation underlies their social navigation capacities. In Study 2, we presented LLMs with a simpler task that does not require any knowledge of multistep social relationships. Using similar methodology as in Study 1, we tested whether LLMs still generate multistep representations in service of this task.

STUDY 1: SOCIAL NAVIGATION

Methods

Large language models

We performed our tests using four open-weight, non-reasoning LLMs: Llama 3.1 (8B), Gemma 3 (12B and 27B), and Mistral Small 3.2 (24B). All LLMs were called programmatically using the open-source Ollama API.

Participants

In analyses directly comparing LLMs with human behavior, we re-analyzed data originally reported in Son et al. (2024) from $N = 146$ participants. All study procedures were conducted in a manner approved by the Brown University Institutional Review Board, and all participants provided informed consent. Further details can be found in the original paper.

Message-passing task

The task was adapted from a social navigation experiment previously tested in humans (Son et al., 2024). In the human experiment, participants first learned about a 13-node artificial social network through trial-and-error feedback, then completed a "message-passing" task (Figure 1A). On each trial, participants were told that a network member wished to send a message to a Target individual, and was required to pass the message to Source A or B (e.g., if Source A were chosen, A would pass the message to one of their friends, who would then pass it to one of *their* friends, and so on until the message reached the Target). The participant's job was to choose the Source who would result in the most efficient delivery. Message-passing problems were designed so that one Source was unambiguously closer to the Target in terms of shortest path distance, and accurate responses were defined as choosing the Source with the shortest path to the Target. Shortest path lengths ranged from 1-3 steps, such that participants could sometimes rely on their knowledge of direct friendships (i.e., for one-step problems), but would otherwise need to mentally navigate across longer distances (i.e., for multistep problems). Participants were never given feedback about the correctness of their responses.

To test LLM social navigation, we converted this task into text prompts (see Figure 1A for an example prompt). We note that our goal was not to create an exact analogue of the human experiment, but to communicate the minimal information necessary for an LLM to perform the task (Frank, 2023). Each prompt presented the full adjacency list of the social network, followed by a message-passing query. LLMs were required to identify and output the correct Source in a single forward pass. To address possible confounds related to real-world statistical co-occurrence between names (e.g., "Jack and Jill" from the English-language nursery rhyme), we created 100 name sets where single-token names were randomly mapped to nodes in the network. Therefore, each LLM was ultimately evaluated on over 5,000 prompts, with variation in both node names and Source-Target pairings. In order to obtain maximally deterministic responses, we set the model temperature to zero. For every prompt, we recorded the model's chosen response (i.e., binary-choice behavior; Figure 1B), as well as the log-probabilities assigned to each of the two candidate Sources (i.e., preference for a Source, given the LLM's network representation; Figure 1B).

Analysis

Binary-choice responses were analyzed using mixed-effects logistic regression implemented in the *glmmTMB* library in *R* (Brooks et al., 2017). Given that each name set was used to generate multiple Source-Target prompts (see previous section), we reasoned that LLM responses to each name set was roughly analogous to a set of responses from one human participant. Responses from each LLM architecture were analyzed in separate regression models.

To characterize the network representations used by LLMs in service of social navigation, we used a form of representational similarity analysis (RSA) to analyze next-token probabilities (Kriegeskorte & Kievit, 2013). For each prompt, the LLM outputs the log-probability of choosing either Source A or B. We used these to compute an LLM preference score, $P_{Correct} - P_{Incorrect}$ (Figure 1B), then compared this preference score to the predictions made by a variety of theoretical models (Figure 1C). We note that we do not analyze LLMs' internal representations in this work; instead, we use LLMs' preferences to infer representation, much as we would infer human representation from behavior.

Theoretical models

Our primary hypothesis was that LLMs represent multistep social relationships. In humans, this is thought to be accomplished by "chaining" one-step associations together, which gives rise to abstracted knowledge of extended relations, i.e., multistep abstraction. Previous work has modeled multistep abstraction in two ways: 1) as a sequential "random walk" process using the Successor Representation (SR) and related models (Dayan, 1993; Lynn et al., 2020; Momennejad et al., 2017;

Son et al., 2023; Son et al., 2024), and 2) as a parallel "spreading activation" process using Katz communicability (Katz, 1953; Teoh et al., 2026; Xia et al., 2025). Mathematically, both variants of multistep abstraction are closely related (Zamora-López & Gilson, 2024), and we test both here. Both models take the following general form, where α controls the amount of memory abstraction (i.e., the number of steps integrated over), and X is a relational matrix containing information about one-step connections between network members:

$$\sum_{k=0}^{\infty} \alpha^k X^k = (I - \alpha X)^{-1}$$

In the SR, $\alpha = \gamma \in (0, 1)$, and $X = T$, the one-step transition matrix. In Katz, $\alpha = \frac{\gamma \in (0,1)}{\lambda}$, where λ is the largest absolute eigenvalue of the adjacency matrix $X = A$. To simplify comparison of these models, we report the multistep "discount" parameter γ, which reflects the proportion of memory abstraction used, and is conceptually interpreted the same way as α. Given a multistep representation, an agent is assumed to prefer the Source with the larger multistep connectivity to the Target (Figure 1C).

To contextualize the strength of representational similarity between LLM representation and multistep models, we also tested how strongly LLM representation corresponds with predictions from a breadth-first search (BFS) graph search algorithm, which has previously been used as a model of both LLM and human planning (Callaway et al., 2022; Correa et al., 2023; Momennejad et al., 2023; Webb et al., 2025). To do so, we drew upon precomputed outputs reported in Son et al. (2024). In brief, this previous work simulated "forward" searches starting from each of the Sources, as well as "backward "searches starting from the Target. We assumed that an agent performing BFS would prefer Sources that tended to appear sooner in a given search (Figure 1C).

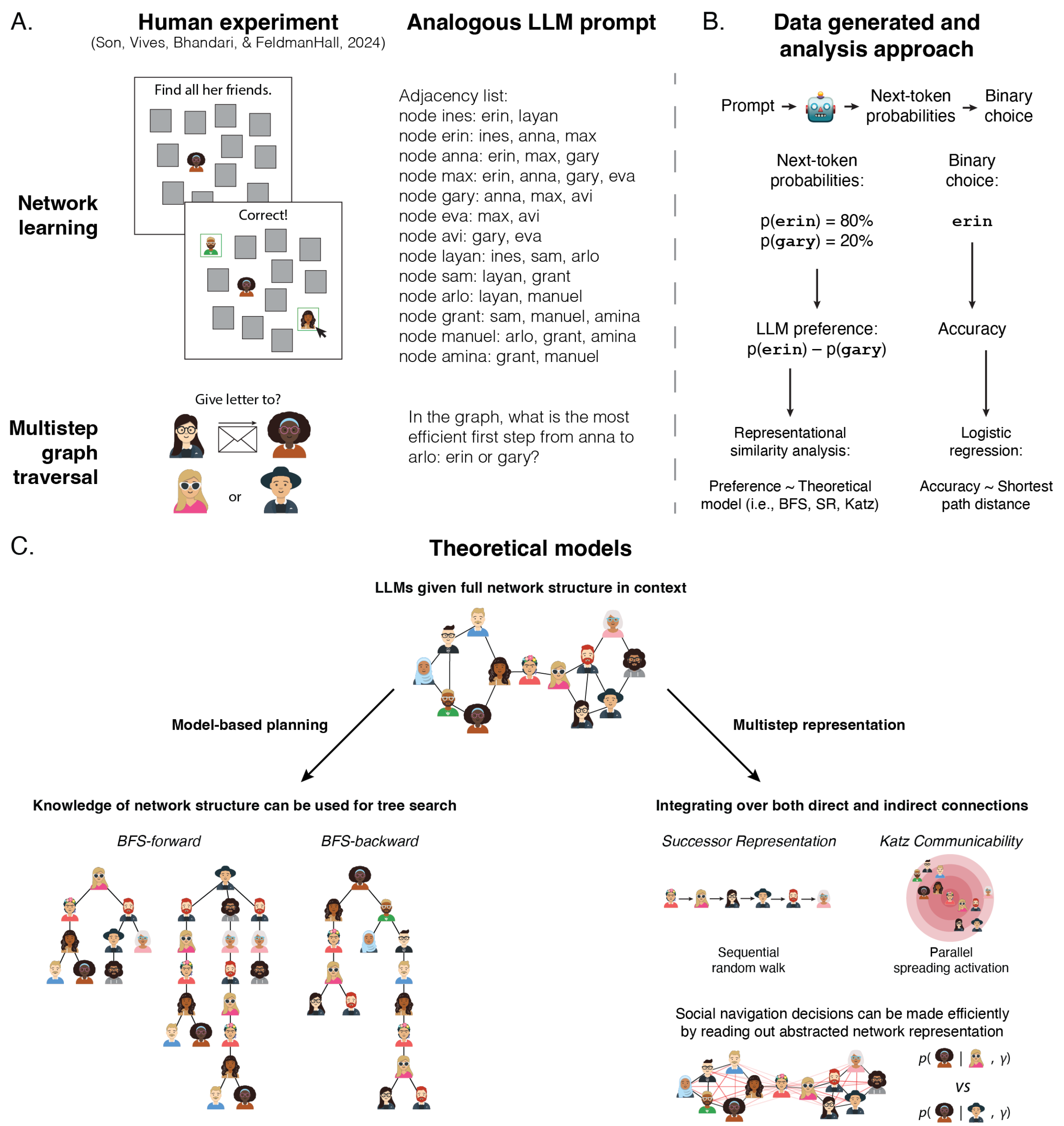

Figure 1 | Conceptual overview of social navigation task. A. *Human social navigation was tested in a previous experiment. Participants learned about an artificial social network from trial-and-error feedback, then were tested on their ability to mentally navigate the social network. The task required participants to deliver a message to a Target individual by choosing between two potential Sources. Each trial contained an unambiguously correct Source, as defined by the shortest path distance between the correct Source and Target, which ranged from 1-3 steps. This social navigation task was adapted into a text prompt for LLMs to solve.* ***B.*** *We recorded two kinds of data from LLMs. First, we recorded next-token probabilities for relevant tokens, which we used to compute an LLM preference score. We used this measure of LLM preference as a proxy for network representation and then used representational similarity analysis to compare LLM representation* *against the predictions made by a variety of theoretical models. Second, we recorded binary choice responses from the LLM, which we used to test behavioral accuracy in the task.* ***C.*** *LLMs were given the full network structure in context. From this, different theoretical models make different predictions about how an LLM might make decisions in the social navigation task. Breadth-first search (BFS) is a form of model-based planning that basically amounts to tree search. Multistep models predict that the agent represents the weighted sum of direct and indirect social connections, over multiple steps of a diffusion process. The Successor Representation (SR) assumes that the diffusion dynamics reflect integration over a sequential random walk. Katz communicability instead models diffusion dynamics as parallel spreading activation.* ***Note.*** *All avatar icons were generated using getavataaars.com, designed by Pablo Stanley and developed by Fang-Pen Lin.*

Results

Navigation accuracy

Previous experiments have demonstrated two defining characteristics of human social navigation using the message-passing task: 1) navigation accuracy is highest for distance-1 problems, and gradually decreases with greater distance; and 2) even for the longest-distance problems tested, people are able to achieve above-chance accuracy (Son et al., 2024). Using binary-choice responses from LLMs, we first tested whether LLM social navigation exhibits these characteristics. Results reveal that all tested LLMs achieve above-chance accuracy, even for the longest path distances (Figure 2A; Table 1), and that LLM navigation accuracy decreases with distance (with the sole exception of Mistral 3.2, where distance-2 accuracy was not significantly different from distance-1 accuracy). Therefore, these results qualitatively mirror patterns observed in human behavior (Figure 2A).

To more precisely quantify similarity between LLM and human choice, we next performed an item analysis comparing LLM and human accuracy for each navigation problem tested. Results reveal that LLMs tend to be more accurate for navigation problems that humans find easier to solve, and less accurate for problems that humans struggle with (Figure 2B; Table 2). This pattern of results emerges across all shortest path distances, with the exception of some distance-1 problems where LLMs exhibit superhuman performance (Figure 2B, estimated means above the dashed line), and therefore exhibit little variability due to having near-ceiling accuracy (Figure 2A).

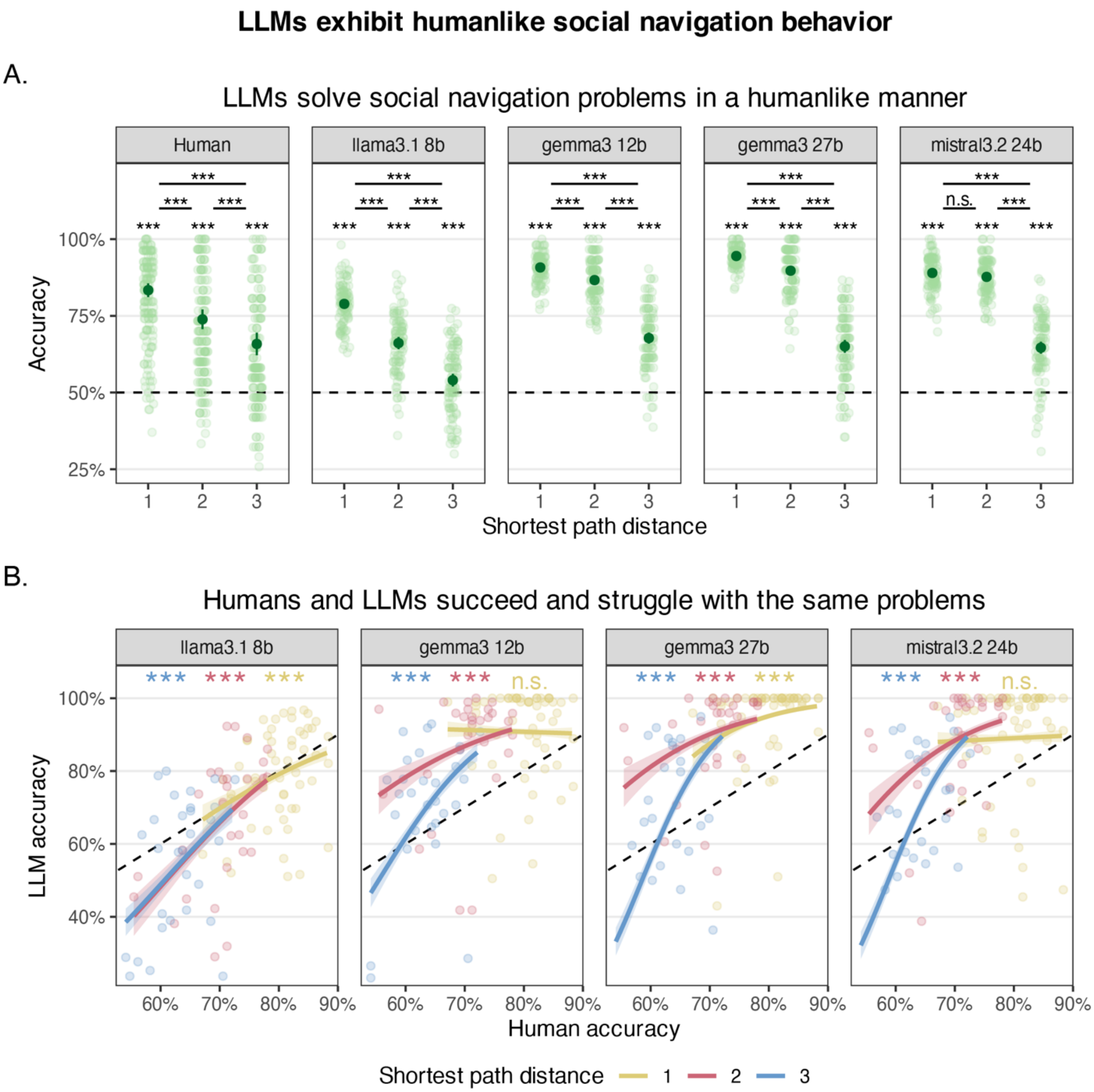

Figure 2 | Social navigation accuracy. A. *Across a variety of LLMs, social navigation accuracy decreases with longer path distances, though accuracy remains above chance across all distances. This qualitatively mirrors human behaviors. We note that the human data have previously been reported in Son et al. (2024), and are only plotted here to serve as a visual reference.* ***B.*** *In an item analysis, human accuracy on a particular problem predicts LLMs' accuracy on that same problem. The dashed line reflects identity; datapoints above this line reflect superhuman performance from LLMs.* ***Note.*** *Error bars/ribbons reflect 95% confidence intervals. * $p < .05$, ** $p < .01$, *** $p < .001$.*

Table 1
LLM social navigation accuracy.

Wilkinson notation: LLM correct choice ~ Shortest path distance						
LLM	**Contrast**	**β est**	**SE**	**Z**	**95% CI**	**p**
llama3.1 8b						
	Dist-1 vs Chance	1.32	0.04	32.73	[1.24, 1.40]	< .001 ***
	Dist-1 vs Dist-2	-0.65	0.05	-12.38	[-0.75, -0.55]	< .001 ***
	Dist-1 vs Dist-3	-1.16	0.05	-22.92	[-1.26, -1.06]	< .001 ***
	Dist-2 vs Chance	0.67	0.04	14.89	[0.58, 0.76]	< .001 ***
	Dist-2 vs Dist-3	-0.51	0.05	-9.35	[-0.61, -0.40]	< .001 ***
	Dist-3 vs Chance	0.16	0.04	3.80	[0.08, 0.24]	< .001 ***
gemma3 12b						
	Dist-1 vs Chance	2.29	0.05	44.77	[2.19, 2.39]	< .001 ***
	Dist-1 vs Dist-2	-0.42	0.07	-5.71	[-0.56, -0.27]	< .001 ***
	Dist-1 vs Dist-3	-1.54	0.06	-24.94	[-1.66, -1.42]	< .001 ***
	Dist-2 vs Chance	1.87	0.06	32.79	[1.76, 1.98]	< .001 ***
	Dist-2 vs Dist-3	-1.13	0.07	-16.85	[-1.26, -1.00]	< .001 ***
	Dist-3 vs Chance	0.74	0.04	17.63	[0.66, 0.83]	< .001 ***
gemma3 27b						
	Dist-1 vs Chance	2.84	0.07	42.22	[2.71, 2.97]	< .001 ***
	Dist-1 vs Dist-2	-0.68	0.09	-7.89	[-0.85, -0.51]	< .001 ***
	Dist-1 vs Dist-3	-2.22	0.07	-30.75	[-2.36, -2.08]	< .001 ***
	Dist-2 vs Chance	2.16	0.07	32.58	[2.03, 2.30]	< .001 ***
	Dist-2 vs Dist-3	-1.54	0.07	-21.60	[-1.68, -1.40]	< .001 ***
	Dist-3 vs Chance	0.62	0.05	13.30	[0.53, 0.71]	< .001 ***
mistral3.2 24b						
	Dist-1 vs Chance	2.09	0.05	41.10	[1.99, 2.19]	< .001 ***
	Dist-1 vs Dist-2	-0.12	0.07	-1.68	[-0.27, 0.02]	.093
	Dist-1 vs Dist-3	-1.49	0.06	-24.63	[-1.60, -1.37]	< .001 ***
	Dist-2 vs Chance	1.96	0.06	31.89	[1.84, 2.08]	< .001 ***
	Dist-2 vs Dist-3	-1.36	0.07	-19.55	[-1.50, -1.23]	< .001 ***
	Dist-3 vs Chance	0.60	0.04	13.84	[0.52, 0.69]	< .001 ***

Note: *Estimates from mixed-effects logistic regression models, with a random intercept per "name set" (see Methods). Tests against "chance" reflect the intercepts of regression models after re-parameterizing the reference category. A separate regression model was fit per LLM.*

Table 2
Item analysis comparing human and LLM social navigation accuracy.

LLM	**Term**	**β est**	**SE**	***Z***	**95% CI**	***p***
llama3.1 8b						
	Human accuracy @ Dist-1	4.95	0.69	7.21	[3.61, 6.30]	< .001 ***
	Human accuracy @ Dist-2	7.26	0.72	10.09	[5.85, 8.67]	< .001 ***
	Human accuracy @ Dist-3	7.16	0.77	9.29	[5.65, 8.67]	< .001 ***
gemma3 12b						
	Human accuracy @ Dist-1	-0.64	0.99	-0.65	[-2.57, 1.29]	.517
	Human accuracy @ Dist-2	6.01	0.90	6.71	[4.25, 7.77]	< .001 ***
	Human accuracy @ Dist-3	10.46	0.83	12.53	[8.82, 12.09]	< .001 ***
gemma3 27b						
	Human accuracy @ Dist-1	10.17	1.18	8.65	[7.87, 12.48]	< .001 ***

LLM	Term	β est	SE	Z	95% CI	p
	Human accuracy @ Dist-2	7.50	0.96	7.78	[5.61, 9.39]	< .001 ***
	Human accuracy @ Dist-3	15.82	0.89	17.86	[14.08, 17.56]	< .001 ***
mistral3.2 24b						
	Human accuracy @ Dist-1	0.79	0.94	0.84	[-1.05, 2.63]	.399
	Human accuracy @ Dist-2	8.72	0.93	9.40	[6.91, 10.54]	< .001 ***
	Human accuracy @ Dist-3	16.00	0.90	17.79	[14.23, 17.76]	< .001 ***

Note: *Estimates from mixed-effects logistic regression models, with a random intercept per "name set" (see Methods), as well as a random slope for human accuracy. A separate regression model was fit per LLM. For brevity, this table only reports tests of the hypothesis that human accuracy for a particular social navigation problem predicts LLM accuracy on that same problem; estimates for each shortest path distance come from re-parameterizing the reference category. The full regression output is reported in Table S1.*

Representational similarity

Even if humans and LLMs exhibit similar social navigation behaviors, this does not imply that humans and LLMs use similar representations to accomplish these behaviors. To test the possibility that LLMs represent social networks in a humanlike manner, we used RSA to compare LLM preferences (i.e., the difference between next-token probabilities for the correct and incorrect answers) against the predictions made by psychologically-plausible theoretical models of multistep abstraction and model-based planning. Past work has demonstrated that humans represent and navigate social networks using multistep abstraction (FeldmanHall et al., 2025; Son et al., 2023; Son et al., 2024; Teoh et al., 2026; Xia et al., 2025), so we reasoned that for LLM preferences to be humanlike, they should be best-explained by multistep models.

We first performed RSA aggregating social navigation problems across all shortest path distances. As expected for a set of psychologically-plausible models, we found that all theoretical models are capable of capturing global patterns in LLM preferences (Table 3; Figure 3A). This is unsurprising, as it likely reflects obvious features of the task, like LLMs having stronger preferences when solving easier single-step problems than when solving harder multistep problems.

To capture finer-grained patterns in LLM preferences, we next performed RSA disaggregating by shortest path distance. In other words, we calculated separate correlation coefficients for distance-1, distance-2, and distance-3 problems. After doing so, results clearly reveal that most theoretical models fail to explain finer-grained patterns of LLM preference. For example, predictions made by the planning models correlate with LLM preferences only weakly, and/or in the wrong direction

(Figure 3B; Table 4). Given that the Successor Representation is a leading model of multistep representation in natural intelligence systems (Gershman, 2018; Momennejad, 2020; Son et al., 2023; Son et al., 2024), it is striking that the SR also systematically fails to explain LLM preferences in this task (Figure 3B; Table 4). Indeed, the *only* theoretical model that reliably correlates with LLM preferences is Katz communicability, with higher γ (i.e., greater multistep integration) correlating most strongly (Figure 3B; Table 4).

As a statistical note, it is perhaps surprising that RSA reveals such a large discrepancy when shortest path distance is (dis)aggregated over. This is known as Simpson's Paradox (Kievit et al., 2013), in which the aggregate trend masks meaningful variability that becomes apparent when the data are appropriately disaggregated. To make this concrete, Figure 3C provides a real example of the correlation between SR preferences and LLM preferences. When aggregating across all shortest path distances, it appears that SR preferences correlate with LLM preferences. However, after disaggregating, it becomes clear that the SR systematically *anti*-correlates with LLM preferences, making it a poor model of LLM representation. We note that the same phenomenon is observed when comparing theoretical models against one another (Figure S1).

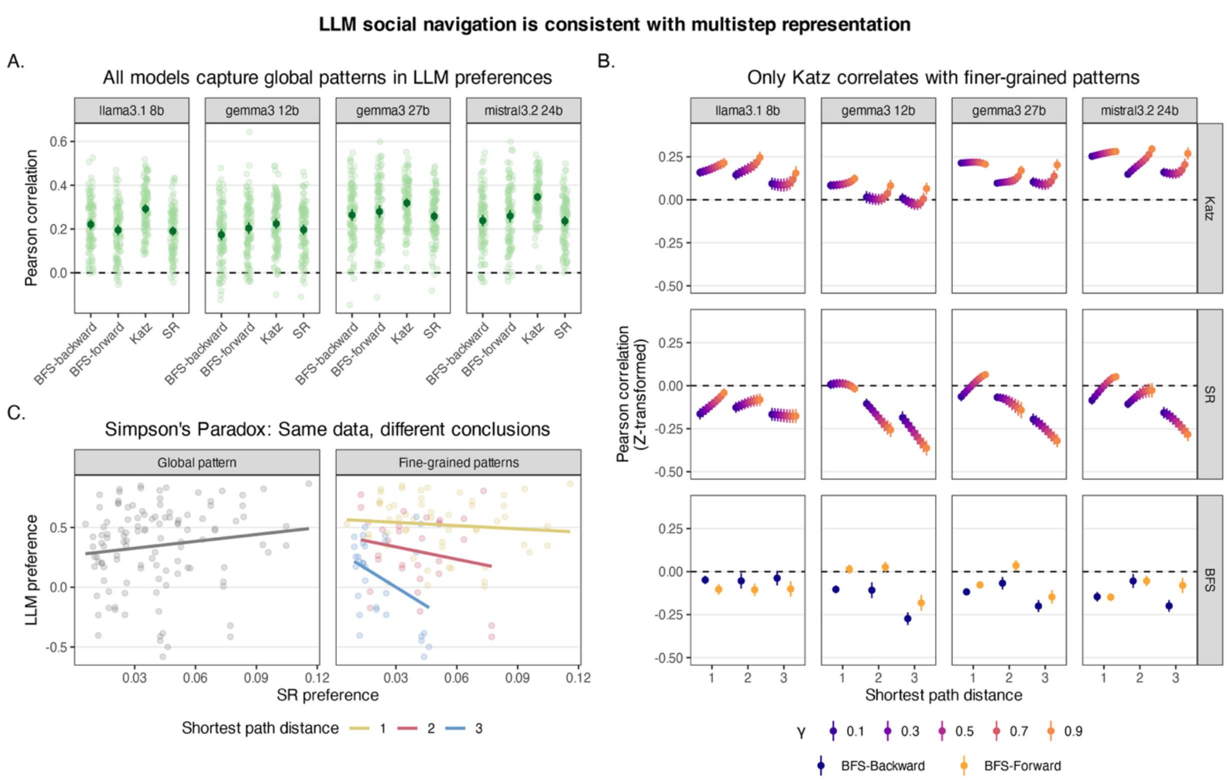

Figure 3 | Representational similarity analysis in the social navigation task. A. *Aggregating across all trials, all theoretical models are able to explain global patterns in LLM preferences.* ***B.*** *After performing disaggregated RSA at each shortest path distance, only Katz multistep representation consistently explains LLM preferences.* ***C.*** *A real example of Simpson's Paradox drawn from our analysis. When aggregating over all trials, there appears to be a positive correlation between the SR model predictions and LLM preference. However, after taking shortest path distance into account, it becomes clear that the SR is actually a poor model of LLM preference.* ***Note.*** ** p < .05, ** p < .01, *** p < .001.*

Table 3

RSA comparing theoretical model predictions against LLM next-token probabilities from the social navigation task, aggregated across all shortest path distances.

LLM	Theoretical model	Mean correlation	*t*	95% CI	*p*
llama3.1 8b					
	BFS-backward	0.22	19.07	[0.20, 0.24]	< .001 ***
	BFS-forward	0.20	16.30	[0.17, 0.22]	< .001 ***
	Katz γ=0.8	0.29	27.06	[0.27, 0.31]	< .001 ***
	SR γ=0.4	0.19	17.68	[0.17, 0.21]	< .001 ***
gemma3 12b					
	BFS-backward	0.17	13.17	[0.15, 0.20]	< .001 ***
	BFS-forward	0.20	15.42	[0.18, 0.23]	< .001 ***
	Katz γ=0.6	0.22	18.42	[0.20, 0.25]	< .001 ***
	SR γ=0.4	0.20	16.70	[0.17, 0.22]	< .001 ***
gemma3 27b					
	BFS-backward	0.26	19.29	[0.24, 0.29]	< .001 ***
	BFS-forward	0.28	19.87	[0.25, 0.31]	< .001 ***
	Katz γ=0.7	0.32	30.81	[0.30, 0.34]	< .001 ***
	SR γ=0.5	0.26	22.94	[0.24, 0.28]	< .001 ***
mistral3.2 24b					
	BFS-backward	0.24	18.47	[0.21, 0.26]	< .001 ***
	BFS-forward	0.26	18.33	[0.23, 0.29]	< .001 ***
	Katz γ=0.8	0.35	35.92	[0.33, 0.37]	< .001 ***
	SR γ=0.6	0.24	20.91	[0.21, 0.26]	< .001 ***

Note: *Second-level t-test results reflect estimated mean Pearson correlations from first-level RSA. For the Katz and SR models, only the results from the "best-fitting" γ are reported.*

Table 4

RSA comparing theoretical model predictions against LLM next-token probabilities from the social navigation task, after disaggregating shortest path distances.

LLM	Theoretical model	Dist-1	Dist-2	Dist-3
llama3.1 8b				
	BFS-backward	-0.05 ***	-0.05 *	-0.04
	BFS-forward	-0.1 ***	-0.11 ***	-0.1 ***
	Katz γ=0.9	0.21 ***	0.25 ***	0.16 ***
	SR γ=0.9	-0.04 **	-0.08 ***	-0.18 ***
gemma3 12b				
	BFS-backward	-0.1 ***	-0.11 ***	-0.27 ***
	BFS-forward	0.01	0.03	-0.18 ***
	Katz γ=0.9	0.12 ***	0.08 ***	0.07 ***

LLM	Theoretical model	Dist-1	Dist-2	Dist-3
	SR γ=0.1	0.01	-0.1 ***	-0.19 ***
gemma3 27b				
	BFS-backward	-0.12 ***	-0.07 ***	-0.2 ***
	BFS-forward	-0.08 ***	0.04 *	-0.15 ***
	Katz γ=0.9	0.21 ***	0.17 ***	0.2 ***
	SR γ=0.3	-0.03	-0.07 ***	-0.22 ***
mistral3.2 24b				
	BFS-backward	-0.15 ***	-0.05 **	-0.2 ***
	BFS-forward	-0.15 ***	-0.05 ***	-0.08 ***
	Katz γ=0.9	0.28 ***	0.29 ***	0.27 ***
	SR γ=0.7	0.03 **	-0.03	-0.24 ***

Note: *Second-level t-test results reflect estimated mean Pearson correlations from first-level RSA, disaggregated by shortest path distance. For the Katz and SR models, only the results from the "best-fitting" γ are reported. An abbreviated table of results is reported here; the full table is reported in Table S2. * p < .05, ** p < .01, *** p < .001.*

Interim Discussion

The results of Study 1 provide evidence that natural and artificial intelligence systems rely on many of the same computational principles to represent and navigate social networks. Indeed, when tasked with the same social navigation problems, LLMs and humans make the same kinds of systematic errors. Like humans, LLMs generate multistep representations that integrate across both direct and indirect connections within the network, which support accurate reasoning about how information flows across a social network. While we have demonstrated that LLMs generate these representations to solve social navigation problems, our first study cannot address whether LLMs—like humans—might also create multistep network representations for tasks that neither require nor benefit from multistep social reasoning.

STUDY 2: NEXT-NODE PREDICTION

Methods

Next-node prediction task

To test whether LLMs spontaneously generate multistep representations for a task where multistep representation is not useful (and may even be harmful), we created a next-node prediction task (Figure 4A). This task is analogous to presenting human participants with a random walk before querying their memory of specific relationships (Pudhiyidath et al., 2022; Schapiro et al., 2013; Son et al., 2023). As in the message-passing task, prompts first presented LLMs with the network's adjacency list. Prompts then listed a random walk ranging from 0-8 steps (where zero steps simply listed a single name), and then asked the LLM to predict the next node in the walk. Because the terminal node's direct connections were already available in-context, multistep representations are not required to predict the next node and may actually harm accuracy by increasing the probability of responding with indirect connections. An example prompt can be found in Figure 4A. To minimize potential confounds related to name co-occurrence, we followed the same procedure as in Study 1 to create randomly-assigned name sets.

Analysis

As in Study 1, we recorded LLMs' log-probabilities for relevant tokens, converted them to probabilities, and used next-token probabilities as a measure of LLM representation (Figure 4A). From the predictions made by the Katz communicability model at $\gamma = [.1, .2, \ldots, .9]$ (Figure 4B), we performed RSA on LLMs' next-token probabilities (Figure 4C).

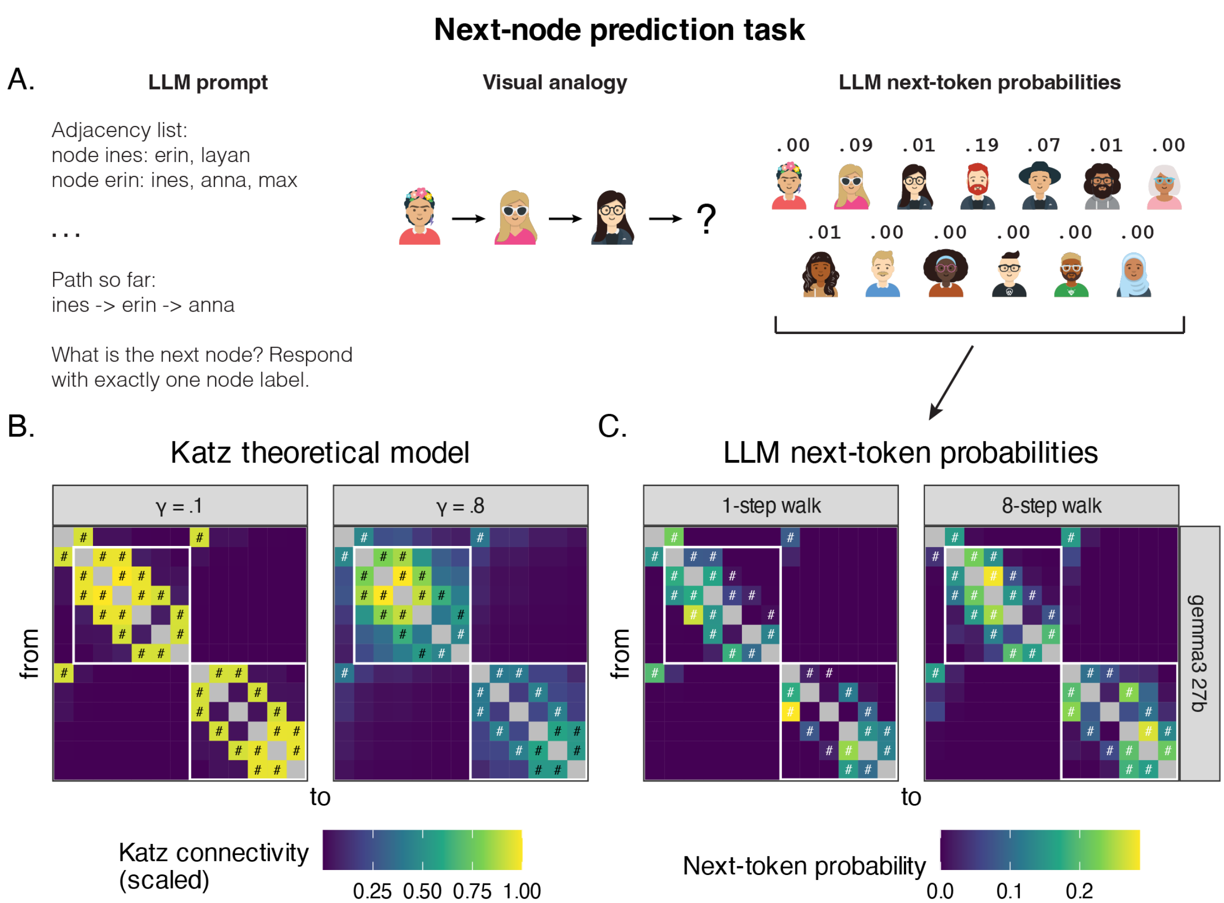

Figure 4 | Conceptual overview of next-node prediction task. A. *The text prompt presented information about a random walk of variable length, then required the LLM to respond with a* *guess about the next node in the walk. To aid conceptual understanding, the visual analogy depicts what a human version of this task might look like. We recorded next-token probabilities for relevant tokens.* ***B.*** *Examples of predicted representations from the Katz communicability model, given low ($\gamma = .1$) and high abstraction ($\gamma = .8$). Hashes indicate true edges. The white boxes mark the two "communities" present in this network.* ***C.*** *Representative examples of LLM next-token probabilities, qualitatively mirroring the predictions made by the theoretical model.*

Results

To maximize prediction accuracy in the next-node prediction task, an optimal strategy is to exclusively represent the terminal node's single-step connections (i.e., direct friendships), without invoking extended knowledge of multistep connections. For an LLM, this would correspond to assigning equal next-token probabilities to the terminal node's friends, and zero probability to all other network members. To see whether LLMs are following this strategy, we first tested whether LLMs' next-token probabilities are better-explained by single-step representation (i.e., $\gamma = 0$), or by multistep representation (i.e., $\gamma > 0$). As a simple form of grid-search parameter-fitting for $\gamma > 0$, we retained only the strongest correlation per name set, per LLM. From this correlation coefficient, we then subtracted the correlation for $\gamma = 0$. Difference scores above zero would therefore provide evidence of multistep representation. Across all tested LLMs, results reveal that next-token probabilities are significantly better-explained by multistep representation than single-step representation (Figure 5A; Table 5). Put simply, in a task that does not require multistep reasoning—and indeed, where multistep representation has a detrimental effect on prediction accuracy—LLMs continue to generate multistep representations.

To better-contextualize our result, we considered several possible alternative interpretations. First, it is possible that LLMs get confused by irrelevant context, such as the non-terminal nodes in the random walk. However, this would not explain why LLMs appear to consistently generate multistep representations, regardless of the length of the random walks and thus the amount of irrelevant context. Indeed, we find evidence of multistep representation even for zero-length random walks, which only consisted of a single name (Figure 5A; Table 5).

Second, from a difference score alone, it remains possible that multistep representations provide a *relatively* better fit compared to single-step representations, while still having an *absolutely* lackluster fit overall. Difference scores also mask the possibility that the multistep model might provide a good fit for longer-range walks, but a poor fit for shorter-length walks, which would limit the generalizability of our results. To address these possibilities, we examined the raw correlation strength between LLM representation and the predicted representation from the best-fitting value of γ (see above). Regardless of random walk length, there were stable and positive correlations between the multistep model and LLM representation (Figure 5B; Table S4), reinforcing our interpretation that LLMs spontaneously generate multistep representations in the next-node prediction task.

Finally, it is possible that the observed correlations are driven by relatively small values of γ. Although this would still provide evidence that LLMs generate multistep representations, it would suggest they are used minimally in the next-node prediction task. Our results instead indicate that LLM representation is best-characterized by moderate values of γ, which holds across LLMs and random walk lengths (Figure 5C; Table S5).

Taken together, these results demonstrate that LLMs spontaneously generate multistep representations of social networks, even when these representations are not needed to solve the task at hand. This mirrors analogous findings in human experiments, which find that people routinely express knowledge of multistep social connections even in experimental contexts where multistep representation is not needed, where people are not tasked with solving social navigation problems, and where accurate behavioral responses are actually harmed by having multistep representations (Son et al., 2023).

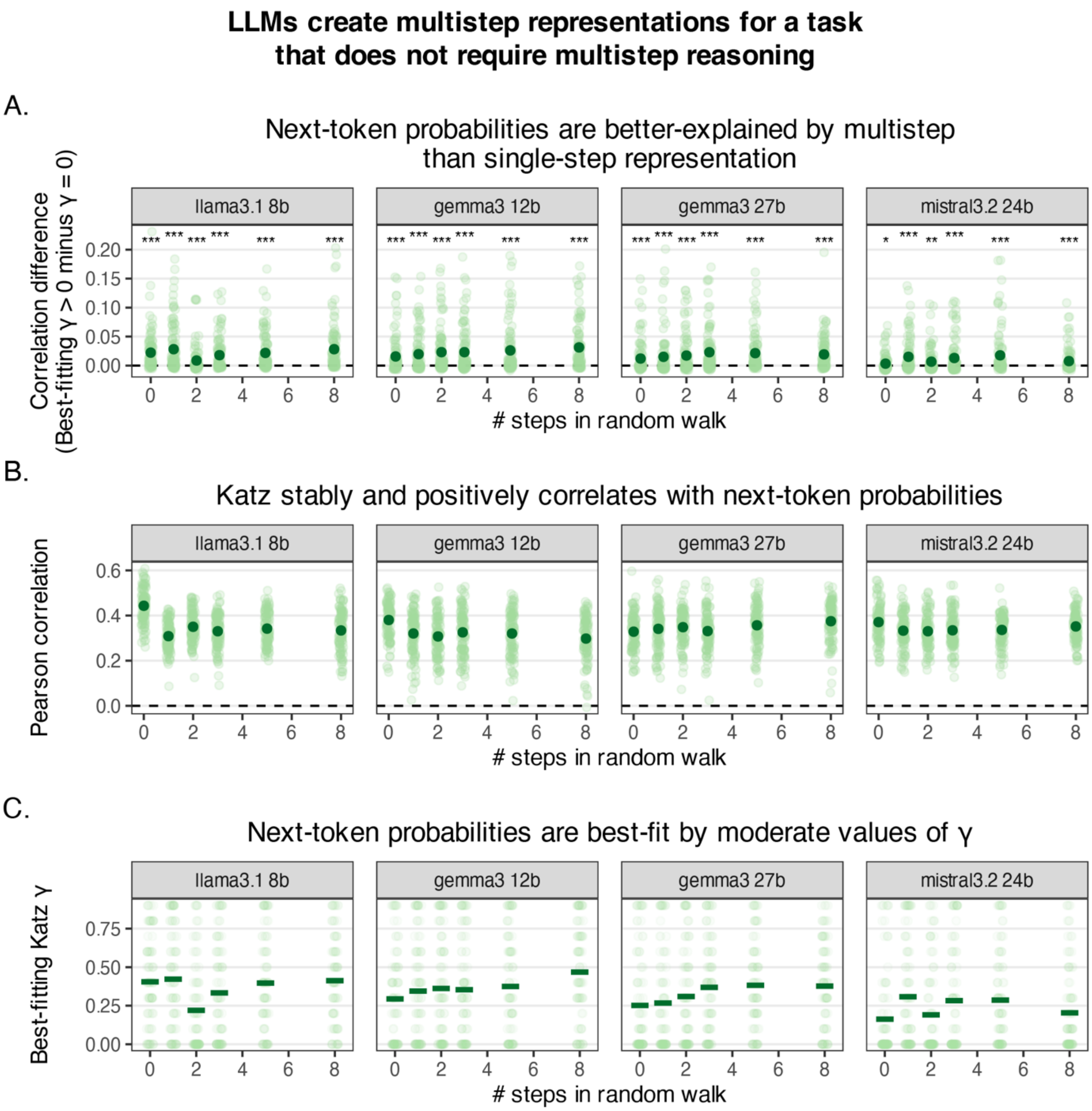

Figure 5 | Representational similarity analysis in the next-node prediction task. A. *LLMs' next-token probabilities are better-explained by multistep representation than single-step representation.* ***B.*** *LLM next-token probabilities are stably and positively correlated with the Katz model of multistep representation.* ***C.*** *Moderate values of γ provide the best fit for next-token probabilities.* ***Note.*** ** p < .05, ** p < .01, *** p < .001.*

Table 5

Testing whether next-token probabilities from the next-node prediction task are better-explained by multistep representation (Katz $\gamma > 0$) or single-step representation.

LLM	0 steps	1 steps	2 steps	3 steps	5 steps	8 steps
llama3.1 8b	0.02 ***	0.03 ***	0.01 ***	0.02 ***	0.02 ***	0.03 ***
gemma3 12b	0.02 ***	0.02 ***	0.02 ***	0.02 ***	0.03 ***	0.03 ***

LLM	0 steps	1 steps	2 steps	3 steps	5 steps	8 steps
gemma3 27b	0.01 ***	0.02 ***	0.02 ***	0.02 ***	0.02 ***	0.02 ***
mistral3.2 24b	0.00 *	0.02 ***	0.01 **	0.01 ***	0.02 ***	0.01 ***

Note: *Results reflect t-tests of the difference between Pearson correlations from first-level RSA using the multistep Katz model, versus single-step edges (i.e.,* $r_{Multistep} - r_{Single-step}$*). Means above zero provide evidence in favor of multistep representation. An abbreviated table of results is reported here; the full table is reported in Table S3. * p < .05, ** p < .01, *** p < .001.*

DISCUSSION

Advances in LLM sophistication have sparked debates about their emergent computational capacities, and how humanlike those capacities are. For now, AI systems continue to struggle with many aspects of social cognition, including theory-of-mind, understanding social and cultural norms, and multi-agent interaction (Mineault et al., 2026; Song et al., 2026; Xu et al., 2025), possibly due to the complexity of the computational processes involved. Our work contributes to this emerging literature by examining an aspect of social cognition—social navigation within an interconnected social network—in which the computational processes involved are likely simpler and shared across many other domains of cognition, and where it is straightforward to test theory-driven hypotheses. Critically, work in cognitive science has produced several well-validated computational models of how humans navigate social networks, allowing us to test not only whether LLMs behave in humanlike ways, but which computational account best explains why.

We find that LLMs are capable of navigating social networks in a way that resembles human social navigation, to the point where humans and LLMs succeed and struggle with the same navigation problems. In both humans and LLMs, this behavioral capacity appears to be supported by abstracted representation of multistep relationships, which integrate over a combination of direct and indirect social connections. In particular, we find that Katz communicability, a model that captures spreading activation dynamics, is the only theoretical model that reliably explains LLM representation. These representations seem not to be task-tailored in LLMs, as we observe evidence that LLMs continue to generate multistep representations in a task where they are neither necessary nor useful. Taken together, our results point to LLMs having the capacity for humanlike representation and navigation of social networks, which might serve as a basic building block for more advanced social cognitive capacities.

Our results speak to a longstanding debate in cognitive science about how multistep representations are computed by biological systems. Most theories assume that multistep representations reflect "in-weight" learning at the time of encoding, and therefore treat multistep representation as a problem of incremental learning from trial-and-error experience (Dayan, 1993; Frank et al., 2003; Gershman et al., 2012; Momennejad et al., 2017; Russek et al., 2017; Schapiro et al., 2013; Son et al., 2023; Son et al., 2024). While it is alternatively possible to generate multistep inferences at retrieval time using recurrent neural networks (RNNs), these models critically depend on recurrence dynamics, like those observed in specific hippocampal circuits (Kumaran & McClelland, 2012; Schapiro et al., 2017). Neither proposal accounts for LLMs' ability to generate multistep representations: LLMs are able to generate multistep representations from a single presentation of the network using "in-context" learning (i.e., without updating model weights), and do so using a feedforward architecture (i.e., without an explicit recurrence mechanism). Nevertheless, LLMs can produce a similar representational signature to humans, suggesting that existing biological theories may have correctly characterized the *output* of multistep representation, without uniquely constraining the *process* by which it is generated. Probing the interactions between in-context and in-weights learning has proven useful for characterizing computational principles shared between humans and artificial intelligence systems (Russin et al., 2025), and a productive avenue for future research will be to examine these interactions with regard to relational representations (Park et al., 2025).

Our findings also make contact with recent mechanistic interpretability work examining how modern AI systems solve problems like multistep reasoning and graph search (Cohen et al., 2025; Park et al., 2025; Saparov et al., 2025; Yang et al., 2024). In contrast to past work, which suggests that edge hallucinations come from in-weights path compression (Dai et al., 2026), we demonstrate here that systematic hallucinations can also be generated through in-context learning of multistep relationships. It is particularly notable that our work points to Katz communicability as the only theoretical model that is able to explain LLM social navigation, as past work has found evidence that LLMs make use of a mechanism resembling parallel spreading activation (Saparov et al., 2025), which is the exact computational principle underlying Katz (Zamora-López & Gilson, 2024). Despite receiving much attention in artificial intelligence and cognitive neuroscience research, our results provide evidence against LLMs using the Successor Representation (SR) to represent social networks. Although the SR is closely related to Katz, it assumes that extended social connections are processed sequentially, rather than in parallel. Given that LLMs' attention mechanism processes token relations in parallel (Vaswani et al., 2017), it is possible that this serves as an inductive bias towards Katz-like representations. Fruitful directions for future work will include careful tests of the algorithmic mechanisms underlying the phenomena reported in our work (Eberle et al., 2025; Lippl et al., 2025).

Future work may also benefit from testing a wider variety of LLMs, task setups, and network structures. Here, we tested only open-weight, non-reasoning LLMs. It remains unknown whether frontier or reasoning-enabled models would show the same multistep signature, or would instead approximate planning-like representations when given the opportunity to reason explicitly. In addition, like most studies comparing humans and LLMs, the two groups necessarily differed in the task setup: humans acquired knowledge of the network through trial-and-error learning, whereas LLMs received a single in-context presentation of the network. Finally, we exclusively tested relatively small (13-node) networks in this work to facilitate direct comparison with previous human experiments. Whether our findings generalize to larger networks with more complex properties remains an open question.

Taken together, our findings show that LLMs represent social networks in a manner that closely mirrors models of human social cognition, allowing LLMs to use knowledge of indirect social connections in service of longer-range social navigation. This multistep representation persists even when it is not required by—and even actively works against—the task at hand. This suggests that multistep abstraction may be a default feature of how LLMs process relational information in-context. Beyond informing debates about how human-like LLM cognition is, these results suggest that LLMs may offer a generative tool for studying computational principles underlying socially-intelligent behavior in both natural and artificial systems.

ACKNOWLEDGEMENTS

We thank members of the Favila Lab, Jake Russin, Michael J. Frank, Ida Momennejad, and three anonymous reviewers at the Cognitive Computational Neuroscience conference for their feedback on this work at previous stages of its development. We thank Alexander Sayette for assistance in implementing earlier versions of the LLM task. We are grateful to Marc-Lluís Vives, Apoorva Bhandari, and Oriel FeldmanHall for making the human dataset available for reanalysis. This work used computational resources supported by the NIH S10 instrumentation grant S10OD036341 (High-Performance Compute Cluster for Brain Science) via the Center for Computation and Visualization (CCV) at Brown University.

REFERENCES

Binz, M., Akata, E., Bethge, M., Brändle, F., Callaway, F., Coda-Forno, J., Dayan, P., Demircan, C., Eckstein, M. K., Éltető, N., Griffiths, T. L., Haridi, S., Jagadish, A. K., Ji-An, L., Kipnis, A., Kumar, S., Ludwig, T., Mathony, M., Mattar, M., . . . Schulz, E. (2025). A foundation model to predict and capture human cognition. *Nature*, *644*(8078), 1002-1009. https://doi.org/10.1038/s41586-025-09215-4

Binz, M., & Schulz, E. (2023). Using cognitive psychology to understand GPT-3. *Proceedings of the National Academy of Sciences*, *120*(6), e2218523120. https://doi.org/10.1073/pnas.2218523120

Brands, R. A. (2013). Cognitive social structures in social network research: A review. *Journal of Organizational Behavior*, *34*(S1), S82-S103. https://doi.org/10.1002/job.1890

Brooks, M. E., Kristensen, K., Van Benthem, K. J., Magnusson, A., Berg, C. W., Nielsen, A., Skaug, H. J., Machler, M., & Bolker, B. M. (2017). glmmTMB balances speed and flexibility among packages for zero-inflated generalized linear mixed modeling. *The R journal*, *9*(2), 378-400.

Callaway, F., van Opheusden, B., Gul, S., Das, P., Krueger, P. M., Griffiths, T. L., & Lieder, F. (2022). Rational use of cognitive resources in human planning. *Nature Human Behaviour*, *6*(8), 1112-1125. https://doi.org/10.1038/s41562-022-01332-8

Cohen, A., Gromov, A., Yang, K., & Tian, Y. (2025). Spectral journey: How transformers predict the shortest path. *arXiv*. https://doi.org/10.48550/arXiv.2502.08794

Correa, C. G., Ho, M. K., Callaway, F., Daw, N. D., & Griffiths, T. L. (2023). Humans decompose tasks by trading off utility and computational cost. *PLOS Computational Biology*, *19*(6), e1011087. https://doi.org/10.1371/journal.pcbi.1011087

Dai, X., Yang, K., Luo, C., Zeng, S., Guo, K., & Tang, J. (2026). When Do Hallucinations Arise? A Graph Perspective on the Evolution of Path Reuse and Path Compression. *arXiv*. https://doi.org/10.48550/arXiv.2604.03557

Dayan, P. (1993). Improving Generalization for Temporal Difference Learning: The Successor Representation. *Neural Computation*, *5*(4), 613-624. https://doi.org/10.1162/neco.1993.5.4.613

Dodds, P. S., Muhamad, R., & Watts, D. J. (2003). An Experimental Study of Search in Global Social Networks. *Science*, *301*(5634), 827. https://doi.org/10.1126/science.1081058

Eberle, O., McGee, T., Giaffar, H., Webb, T., & Momennejad, I. (2025). Position: We need an algorithmic understanding of generative AI. *arXiv*. https://doi.org/10.48550/arXiv.2510.15987

FeldmanHall, O., Son, J.-Y., & Bhandari, A. (2025). Abstract Cognitive Maps for Complex Social Systems. *Current Directions in Psychological Science*, 09637214251342742. https://doi.org/10.1177/09637214251342742

Frank, M. C. (2023). Baby steps in evaluating the capacities of large language models. *Nature Reviews Psychology*, *2*(8), 451-452. https://doi.org/10.1038/s44159-023-00211-x

Frank, M. J., Rudy, J. W., & O'Reilly, R. C. (2003). Transitivity, flexibility, conjunctive representations, and the hippocampus. II. A computational analysis. *Hippocampus*, *13*(3), 341-354. https://doi.org/https://doi.org/10.1002/hipo.10084

Gershman, S. J. (2018). The Successor Representation: Its Computational Logic and Neural Substrates. *The Journal of Neuroscience*, *38*(33), 7193. https://doi.org/10.1523/JNEUROSCI.0151-18.2018

Gershman, S. J., Moore, C. D., Todd, M. T., Norman, K. A., & Sederberg, P. B. (2012). The Successor Representation and Temporal Context. *Neural Computation*, *24*(6), 1553-1568. https://doi.org/10.1162/NECO_a_00282

Griffiths, T. L. (2020). Understanding Human Intelligence through Human Limitations. *Trends in Cognitive Sciences*, *24*(11), 873-883. https://doi.org/10.1016/j.tics.2020.09.001

Katz, L. (1953). A new status index derived from sociometric analysis. *Psychometrika*, *18*(1), 39-43. https://doi.org/10.1007/BF02289026

Kievit, R., Frankenhuis, W. E., Waldorp, L., & Borsboom, D. (2013). Simpson's paradox in psychological science: a practical guide [Hypothesis and Theory]. *Frontiers in Psychology*, *Volume 4 - 2013*. https://www.frontiersin.org/journals/psychology/articles/10.3389/fpsyg.2013.00513

Krackhardt, D. (1987). Cognitive social structures. *Social Networks*, *9*(2), 109-134. https://doi.org/https://doi.org/10.1016/0378-8733(87)90009-8

Kriegeskorte, N., & Kievit, R. A. (2013). Representational geometry: integrating cognition, computation, and the brain. *Trends in Cognitive Sciences*, *17*(8), 401-412. https://doi.org/10.1016/j.tics.2013.06.007

Kumaran, D., & McClelland, J. L. (2012). Generalization through the recurrent interaction of episodic memories: A model of the hippocampal system. *Psychological Review*, *119*(3), 573-616. https://doi.org/10.1037/a0028681

Lieder, F., & Griffiths, T. L. (2020). Resource-rational analysis: Understanding human cognition as the optimal use of limited computational resources. *Behavioral and Brain Sciences*, *43*, e1, Article e1. https://doi.org/10.1017/S0140525X1900061X

Lippl, S., McGee, T., Lopez, K., Pan, Z., Zhang, P., Ziadi, S., Eberle, O., & Momennejad, I. (2025). Algorithmic primitives and compositional geometry of reasoning in language models. *arXiv*. https://doi.org/10.48550/arXiv.2510.15987

Lynn, C. W., & Bassett, D. S. (2020). How humans learn and represent networks. *Proceedings of the National Academy of Sciences*, *117*(47), 29407. https://doi.org/10.1073/pnas.1912328117

Lynn, C. W., Kahn, A. E., Nyema, N., & Bassett, D. S. (2020). Abstract representations of events arise from mental errors in learning and memory. *Nature Communications*, *11*(1), 2313. https://doi.org/10.1038/s41467-020-15146-7

Mineault, P. J., Griffiths, T. L., & Escola, S. (2026). Cognitive dark matter: Measuring what ai misses. *arXiv*. https://doi.org/10.48550/arXiv.2603.03414

Momennejad, I. (2020). Learning Structures: Predictive Representations, Replay, and Generalization. *Current Opinion in Behavioral Sciences*, *32*, 155-166. https://doi.org/https://doi.org/10.1016/j.cobeha.2020.02.017

Momennejad, I. (2021). Collective minds: social network topology shapes collective cognition. *Philosophical Transactions of the Royal Society B: Biological Sciences*, *377*(1843), 20200315. https://doi.org/10.1098/rstb.2020.0315

Momennejad, I., Hasanbeig, H., Vieira Frujeri, F., Sharma, H., Jojic, N., Palangi, H., Ness, R., & Larson, J. (2023). Evaluating cognitive maps and planning in large language models with cogeval. *Advances in neural information processing systems*, *36*, 69736-69751. https://doi.org/10.48550/arXiv.2309.15129

Momennejad, I., Russek, E. M., Cheong, J. H., Botvinick, M. M., Daw, N. D., & Gershman, S. J. (2017). The successor representation in human reinforcement learning. *Nature Human Behaviour*, *1*(9), 680-692. https://doi.org/10.1038/s41562-017-0180-8

Park, C. F., Lee, A., Lubana, E. S., Yang, Y., Okawa, M., Nishi, K., Wattenberg, M., & Tanaka, H. (2025). ICLR: In-context learning of representations. International Conference on Learning Representations.

Pudhiyidath, A., Morton, N. W., Duran, R. V., Schapiro, A. C., Momennejad, I., Hinojosa-Rowland, D. M., Molitor, R. J., & Preston, A. R. (2022). Representations of Temporal Community Structure in Hippocampus and Precuneus Predict Inductive Reasoning Decisions. *Journal of Cognitive Neuroscience*, 1-25. https://doi.org/10.1162/jocn_a_01864

Russek, E. M., Momennejad, I., Botvinick, M. M., Gershman, S. J., & Daw, N. D. (2017). Predictive representations can link model-based reinforcement learning to model-free mechanisms. *PLOS Computational Biology*, *13*(9), e1005768. https://doi.org/10.1371/journal.pcbi.1005768

Russin, J., Pavlick, E., & Frank, M. J. (2025). Parallel trade-offs in human cognition and neural networks: The dynamic interplay between in-context and in-weight learning. *Proceedings of the National Academy of Sciences*, *122*(35), e2510270122. https://doi.org/10.1073/pnas.2510270122

Saparov, A., Pawar, S. A., Pimpalgaonkar, S., Joshi, N., Pang, R. Y., Padmakumar, V., Kazemi, S. M., Kim, N., & He, H. (2025). Transformers struggle to learn to search.

Schapiro, A. C., Rogers, T. T., Cordova, N. I., Turk-Browne, N. B., & Botvinick, M. M. (2013). Neural representations of events arise from temporal community structure. *Nature Neuroscience*, *16*(4), 486-492. https://doi.org/10.1038/nn.3331

Schapiro, A. C., Turk-Browne, N. B., Botvinick, M. M., & Norman, K. A. (2017). Complementary learning systems within the hippocampus: a neural network modelling approach to reconciling episodic memory with statistical learning. *Philosophical Transactions of the Royal Society B: Biological Sciences*, *372*(1711), 20160049. https://doi.org/10.1098/rstb.2016.0049

Smith, E. B., Brands, R. A., Brashears, M. E., & Kleinbaum, A. M. (2020). Social Networks and Cognition. *Annual Review of Sociology*, *46*(1), 159-174. https://doi.org/10.1146/annurev-soc-121919-054736

Son, J.-Y., Bhandari, A., & FeldmanHall, O. (2023). Abstract cognitive maps of social network structure aid adaptive inference. *Proceedings of the National Academy of Sciences*, *120*(47), e2310801120. https://doi.org/10.1073/pnas.2310801120

Son, J.-Y., Vives, M.-L., Bhandari, A., & FeldmanHall, O. (2024). Replay shapes abstract cognitive maps for efficient social navigation. *Nature Human Behaviour*. https://doi.org/10.1038/s41562-024-01990-w

Song, P., Han, P., & Goodman, N. (2026). Large language model reasoning failures. *arXiv*. https://doi.org/10.48550/arXiv.2602.06176

Teoh, Y. Y., Son, J.-Y., Xia, A., Bhandari, A., & FeldmanHall, O. (2026). Medial temporal lobe encodes cognitive maps of real-world social networks. *Proceedings of the National Academy of Sciences*, *123*(16), e2523345123. https://doi.org/10.1073/pnas.2523345123

Travers, J., & Milgram, S. (1969). An Experimental Study of the Small World Problem. *Sociometry*, *32*(4), 425-443. https://doi.org/10.2307/2786545

Vaswani, A., Shazeer, N., Parmar, N., Uszkoreit, J., Jones, L., Gomez, A. N., Kaiser, Ł., & Polosukhin, I. (2017). Attention is all you need. *Advances in neural information processing systems*, *30*. https://doi.org/10.48550/arXiv.1706.03762

Webb, T., Mondal, S. S., & Momennejad, I. (2025). A brain-inspired agentic architecture to improve planning with LLMs. *Nature Communications*, *16*(1), 8633. https://doi.org/10.1038/s41467-025-63804-5

Xia, A., Teoh, Y. Y., Nassar, M. R., Bhandari, A., & FeldmanHall, O. (2025). Knowledge of information cascades through social networks facilitates strategic gossip. *Nature Human Behaviour*. https://doi.org/10.1038/s41562-025-02241-2

Xu, Z., Wang, Y., Huang, Y., Ye, J., Zhuang, H., Song, Z., Gao, L., Wang, C., Chen, Z., & Zhou, Y. (2025). Socialmaze: A benchmark for evaluating social reasoning in large language models. *arXiv*. https://doi.org/10.48550/arXiv.2505.23713

Yamada, Y., Bao, Y., Lampinen, A. K., Kasai, J., & Yildirim, I. (2023). Evaluating spatial understanding of large language models. *arXiv*. https://doi.org/10.48550/arXiv.2310.14540

Yang, S., Gribovskaya, E., Kassner, N., Geva, M., & Riedel, S. (2024). Do large language models latently perform multi-hop reasoning?

Zamora-López, G., & Gilson, M. (2024). An integrative dynamical perspective for graph theory and the analysis of complex networks. *Chaos: An Interdisciplinary Journal of Nonlinear Science*, *34*(4), 041501. https://doi.org/10.1063/5.0202241

Supplementary Information
Humanlike representation of social networks in large language models

Jae-Young Son[1,2*], Daniel L. Carstensen[1,3*], & Serra E. Favila[1,2]

[1] Department of Cognitive & Psychological Sciences, Brown University
[2] Robert J. and Nancy D. Carney Institute for Brain Science, Brown University
[3] Current Address: Department of Psychology, University of Pennsylvania
* Equal contribution

Corresponding Authors:
Jae-Young Son (jae@brown.edu) & Serra E. Favila (serra_favila@brown.edu)

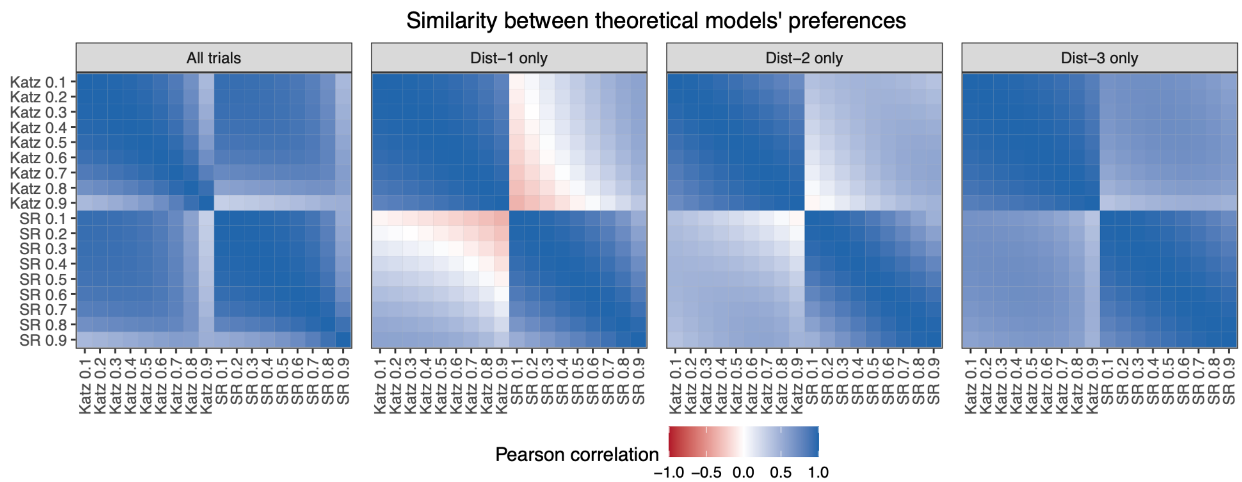

Figure S1 | Pearson correlations between multistep models' preferences in the social navigation task. *When aggregating across all trials, the Katz communicability and Successor Representation (SR) models appear to have highly similar preferences. However, disaggregating by shortest path distance reveals finer-grained differences in their preferences, including (in some cases)* ***anti****-correlation between models.*

Table S1

Item analysis comparing human and LLM social navigation accuracy.

LLM	Reference category	Term	β est	SE	Z	95% CI	p
llama3.1 8b							
	Dist-1						
		(Intercept)	-2.63	0.55	-4.81	[-3.70, -1.56]	< .001 ***
		Human accuracy	4.95	0.69	7.21	[3.61, 6.30]	< .001 ***
		Dist-2	-1.79	0.74	-2.41	[-3.25, -0.34]	.016 *
		Dist-3	-1.71	0.73	-2.34	[-3.14, -0.28]	.019 *
		Human accuracy × Dist-2	2.31	0.99	2.32	[0.36, 4.26]	.02 *
		Human accuracy × Dist-3	2.21	1.03	2.14	[0.18, 4.23]	.032 *
llama3.1 8b							
	Dist-2						
		(Intercept)	-4.43	0.51	-8.76	[-5.42, -3.44]	< .001 ***
		Human accuracy	7.26	0.72	10.09	[5.85, 8.67]	< .001 ***
		Dist-1	1.79	0.74	2.41	[0.34, 3.25]	.016 *
		Dist-3	0.08	0.70	0.12	[-1.29, 1.46]	.904
		Human accuracy × Dist-1	-2.31	0.99	-2.32	[-4.26, -0.36]	.02 *
		Human accuracy × Dist-3	-0.10	1.05	-0.10	[-2.17, 1.96]	.923
llama3.1 8b							
	Dist-3						
		(Intercept)	-4.34	0.49	-8.93	[-5.29, -3.39]	< .001 ***
		Human accuracy	7.16	0.77	9.29	[5.65, 8.67]	< .001 ***
		Dist-1	1.71	0.73	2.34	[0.28, 3.14]	.019 *
		Dist-2	-0.08	0.70	-0.12	[-1.46, 1.29]	.904
		Human accuracy × Dist-1	-2.21	1.03	-2.14	[-4.23, -0.18]	.032 *
		Human accuracy × Dist-2	0.10	1.05	0.10	[-1.96, 2.17]	.923
gemma3 12b							
	Dist-1						
		(Intercept)	2.80	0.79	3.53	[1.25, 4.35]	< .001 ***
		Human accuracy	-0.64	0.99	-0.65	[-2.57, 1.29]	.517
		Dist-2	-5.12	1.01	-5.09	[-7.09, -3.15]	< .001 ***
		Dist-3	-8.59	0.95	-9.07	[-10.45, -6.74]	< .001 ***
		Human accuracy × Dist-2	6.65	1.33	4.99	[4.04, 9.26]	< .001 ***

LLM	Reference category	Term	*β* est	SE	*Z*	95% CI	*p*
		Human accuracy × Dist-3	11.10	1.29	8.59	[8.56, 13.63]	< .001 ***
gemma3 12b							
	Dist-2						
		(Intercept)	-2.32	0.62	-3.73	[-3.54, -1.10]	< .001 ***
		Human accuracy	6.01	0.90	6.71	[4.25, 7.77]	< .001 ***
		Dist-1	5.12	1.01	5.09	[3.15, 7.09]	< .001 ***
		Dist-3	-3.47	0.81	-4.29	[-5.06, -1.89]	< .001 ***
		Human accuracy × Dist-1	-6.65	1.33	-4.99	[-9.26, -4.04]	< .001 ***
		Human accuracy × Dist-3	4.45	1.22	3.63	[2.05, 6.85]	< .001 ***
gemma3 12b							
	Dist-3						
		(Intercept)	-5.80	0.52	-11.14	[-6.82, -4.78]	< .001 ***
		Human accuracy	10.46	0.83	12.53	[8.82, 12.09]	< .001 ***
		Dist-1	8.59	0.95	9.07	[6.74, 10.45]	< .001 ***
		Dist-2	3.47	0.81	4.29	[1.89, 5.06]	< .001 ***
		Human accuracy × Dist-1	-11.10	1.29	-8.59	[-13.63, -8.56]	< .001 ***
		Human accuracy × Dist-2	-4.45	1.22	-3.63	[-6.85, -2.05]	< .001 ***
gemma3 27b							
	Dist-1						
		(Intercept)	-5.17	0.92	-5.64	[-6.97, -3.38]	< .001 ***
		Human accuracy	10.17	1.18	8.65	[7.87, 12.48]	< .001 ***
		Dist-2	2.13	1.13	1.88	[-0.09, 4.35]	.059
		Dist-3	-4.09	1.07	-3.82	[-6.18, -1.99]	< .001 ***
		Human accuracy × Dist-2	-2.67	1.52	-1.76	[-5.65, 0.31]	.079
		Human accuracy × Dist-3	5.65	1.47	3.84	[2.76, 8.53]	< .001 ***
gemma3 27b							
	Dist-2						
		(Intercept)	-3.04	0.66	-4.58	[-4.34, -1.74]	< .001 ***
		Human accuracy	7.50	0.96	7.78	[5.61, 9.39]	< .001 ***
		Dist-1	-2.13	1.13	-1.89	[-4.35, 0.08]	.059
		Dist-3	-6.22	0.86	-7.21	[-7.91, -4.53]	< .001 ***

LLM	Reference category	Term	*β* est	SE	*Z*	95% CI	*p*
		Human accuracy × Dist-1	2.67	1.52	1.76	[-0.31, 5.65]	.079
		Human accuracy × Dist-3	8.32	1.31	6.36	[5.76, 10.89]	< .001 ***
gemma3 27b							
	Dist-3						
		(Intercept)	-9.26	0.55	-16.79	[-10.34, -8.18]	< .001 ***
		Human accuracy	15.82	0.89	17.86	[14.08, 17.56]	< .001 ***
		Dist-1	4.09	1.07	3.82	[1.99, 6.18]	< .001 ***
		Dist-2	6.22	0.86	7.21	[4.53, 7.91]	< .001 ***
		Human accuracy × Dist-1	-5.65	1.47	-3.84	[-8.53, -2.76]	< .001 ***
		Human accuracy × Dist-2	-8.32	1.31	-6.36	[-10.89, -5.76]	< .001 ***
mistral3.2 24b							
	Dist-1						
		(Intercept)	1.46	0.75	1.95	[-0.01, 2.93]	.052
		Human accuracy	0.79	0.94	0.84	[-1.05, 2.63]	.399
		Dist-2	-5.54	0.98	-5.63	[-7.46, -3.61]	< .001 ***
		Dist-3	-10.86	0.94	-11.60	[-12.70, -9.03]	< .001 ***
		Human accuracy × Dist-2	7.93	1.32	6.01	[5.35, 10.52]	< .001 ***
		Human accuracy × Dist-3	15.20	1.30	11.70	[12.66, 17.75]	< .001 ***
mistral3.2 24b							
	Dist-2						
		(Intercept)	-4.08	0.64	-6.40	[-5.32, -2.83]	< .001 ***
		Human accuracy	8.72	0.93	9.40	[6.91, 10.54]	< .001 ***
		Dist-1	5.54	0.98	5.63	[3.61, 7.46]	< .001 ***
		Dist-3	-5.32	0.85	-6.29	[-6.98, -3.66]	< .001 ***
		Human accuracy × Dist-1	-7.93	1.32	-6.01	[-10.52, -5.35]	< .001 ***
		Human accuracy × Dist-3	7.27	1.29	5.63	[4.74, 9.80]	< .001 ***
mistral3.2 24b							
	Dist-3						
		(Intercept)	-9.40	0.56	-16.78	[-10.50, -8.30]	< .001 ***

LLM	Reference category	Term	*β* est	SE	*Z*	95% CI	*p*
		Human accuracy	16.00	0.90	17.79	[14.23, 17.76]	< .001 ***
		Dist-1	10.86	0.94	11.60	[9.03, 12.70]	< .001 ***
		Dist-2	5.32	0.85	6.29	[3.66, 6.98]	< .001 ***
		Human accuracy × Dist-1	-15.20	1.30	-11.70	[-17.75, -12.66]	< .001 ***
		Human accuracy × Dist-2	-7.27	1.29	-5.63	[-9.80, -4.74]	< .001 ***

Note: *Estimates from mixed-effects logistic regression models, with a random intercept per "name set" (see Methods), as well as a random slope for human accuracy. A separate regression model was fit per LLM.*

Table S2
RSA comparing theoretical model predictions against LLM next-token probabilities from the social navigation task, after disaggregating shortest path distances.

LLM	Theoretical model	Shortest path distance	Mean correlation	*t*	95% CI	*p*
llama3.1 8b						
	BFS-backward					
		1	-0.05	-4.06	[-0.07, -0.02]	< .001 ***
		2	-0.05	-2.36	[-0.10, -0.01]	.02 *
		3	-0.04	-1.79	[-0.08, 0.00]	.076
llama3.1 8b						
	BFS-forward					
		1	-0.10	-6.71	[-0.13, -0.07]	< .001 ***
		2	-0.11	-5.77	[-0.14, -0.07]	< .001 ***
		3	-0.10	-4.47	[-0.15, -0.06]	< .001 ***
llama3.1 8b						
	Katz γ=0.9					
		1	0.21	14.73	[0.19, 0.24]	< .001 ***
		2	0.25	14.23	[0.21, 0.28]	< .001 ***
		3	0.16	7.66	[0.11, 0.20]	< .001 ***
llama3.1 8b						
	SR γ=0.9					
		1	-0.04	-3.22	[-0.07, -0.02]	.002 **
		2	-0.08	-4.54	[-0.12, -0.05]	< .001 ***
		3	-0.18	-8.64	[-0.22, -0.14]	< .001 ***
gemma3 12b						
	BFS-backward					
		1	-0.10	-9.03	[-0.13, -0.08]	< .001 ***
		2	-0.11	-4.70	[-0.15, -0.06]	< .001 ***
		3	-0.27	-14.83	[-0.31, -0.24]	< .001 ***
gemma3 12b						
	BFS-forward					
		1	0.01	1.10	[-0.01, 0.04]	.273
		2	0.03	1.75	[-0.00, 0.06]	.083

LLM	Theoretical model	Shortest path distance	Mean correlation	*t*	95% CI	*p*
		3	-0.18	-7.88	[-0.23, -0.14]	< .001 ***
gemma3 12b						
	Katz γ=0.9					
		1	0.12	9.95	[0.10, 0.15]	< .001 ***
		2	0.08	4.93	[0.05, 0.12]	< .001 ***
		3	0.07	3.63	[0.03, 0.10]	< .001 ***
gemma3 12b						
	SR γ=0.1					
		1	0.01	0.52	[-0.02, 0.03]	.605
		2	-0.10	-7.06	[-0.13, -0.08]	< .001 ***
		3	-0.19	-10.09	[-0.22, -0.15]	< .001 ***
gemma3 27b						
	BFS-backward					
		1	-0.12	-12.32	[-0.14, -0.10]	< .001 ***
		2	-0.07	-3.67	[-0.10, -0.03]	< .001 ***
		3	-0.20	-11.61	[-0.23, -0.17]	< .001 ***
gemma3 27b						
	BFS-forward					
		1	-0.08	-7.18	[-0.10, -0.06]	< .001 ***
		2	0.04	2.19	[0.00, 0.07]	.031 *
		3	-0.15	-7.45	[-0.19, -0.11]	< .001 ***
gemma3 27b						
	Katz γ=0.9					
		1	0.21	27.24	[0.19, 0.22]	< .001 ***
		2	0.17	12.31	[0.14, 0.20]	< .001 ***
		3	0.20	11.98	[0.17, 0.24]	< .001 ***
gemma3 27b						
	SR γ=0.3					
		1	-0.03	-1.88	[-0.05, 0.00]	.063
		2	-0.07	-5.61	[-0.10, -0.05]	< .001 ***
		3	-0.22	-12.47	[-0.25, -0.18]	< .001 ***
mistral3.2 24b						
	BFS-backward					

LLM	Theoretical model	Shortest path distance	Mean correlation	*t*	95% CI	*p*
		1	-0.15	-10.69	[-0.17, -0.12]	< .001 ***
		2	-0.05	-2.64	[-0.10, -0.01]	.01 **
		3	-0.20	-11.69	[-0.23, -0.17]	< .001 ***
mistral3.2 24b						
	BFS-forward					
		1	-0.15	-13.05	[-0.17, -0.13]	< .001 ***
		2	-0.05	-3.58	[-0.08, -0.02]	< .001 ***
		3	-0.08	-3.61	[-0.12, -0.04]	< .001 ***
mistral3.2 24b						
	Katz γ=0.9					
		1	0.28	31.41	[0.26, 0.30]	< .001 ***
		2	0.29	26.71	[0.27, 0.32]	< .001 ***
		3	0.27	15.51	[0.23, 0.30]	< .001 ***
mistral3.2 24b						
	SR γ=0.7					
		1	0.03	3.05	[0.01, 0.06]	.003 **
		2	-0.03	-1.60	[-0.07, 0.01]	.114
		3	-0.24	-12.76	[-0.28, -0.21]	< .001 ***

Note: *Second-level t-test results reflect estimated mean Pearson correlations from first-level RSA, disaggregated by shortest path distance. For the Katz and SR models, only the results from the "best-fitting" γ are reported.*

Table S3

Testing whether next-token probabilities from the next-node prediction task are better-explained by multistep representation (Katz $\gamma > 0$) or single-step representation.

LLM	# steps	Mean corr. diff.	*t*	95% CI	*p*
llama3.1 8b					
	0	0.02	6.64	[0.02, 0.03]	< .001 ***
	1	0.03	6.80	[0.02, 0.04]	< .001 ***
	2	0.01	3.55	[0.00, 0.01]	< .001 ***
	3	0.02	6.22	[0.01, 0.02]	< .001 ***
	5	0.02	6.75	[0.02, 0.03]	< .001 ***
	8	0.03	6.75	[0.02, 0.04]	< .001 ***
gemma3 12b					
	0	0.02	4.73	[0.01, 0.02]	< .001 ***
	1	0.02	6.06	[0.01, 0.03]	< .001 ***
	2	0.02	5.99	[0.02, 0.03]	< .001 ***
	3	0.02	5.83	[0.02, 0.03]	< .001 ***
	5	0.03	5.99	[0.02, 0.03]	< .001 ***
	8	0.03	7.66	[0.02, 0.04]	< .001 ***
gemma3 27b					
	0	0.01	4.14	[0.01, 0.02]	< .001 ***
	1	0.02	4.04	[0.01, 0.02]	< .001 ***
	2	0.02	5.28	[0.01, 0.02]	< .001 ***
	3	0.02	6.09	[0.02, 0.03]	< .001 ***
	5	0.02	6.40	[0.01, 0.03]	< .001 ***
	8	0.02	6.87	[0.01, 0.02]	< .001 ***
mistral3.2 24b					
	0	0.00	2.31	[0.00, 0.01]	.023 *
	1	0.02	5.16	[0.01, 0.02]	< .001 ***
	2	0.01	3.18	[0.00, 0.01]	.002 **
	3	0.01	4.41	[0.01, 0.02]	< .001 ***
	5	0.02	4.54	[0.01, 0.03]	< .001 ***
	8	0.01	3.70	[0.00, 0.01]	< .001 ***

Note: *Results reflect t-tests of the difference between Pearson correlations from first-level RSA using the multistep Katz model, versus single-step edges (i.e., $r_{Multistep} - r_{Single-step}$). Means above zero provide evidence in favor of multistep representation.*

Table S4

Correlations between next-token probabilities from the next-node prediction task, and the Katz model of multistep representation.

LLM	# steps	Mean corr.	*t*	95% CI	*p*
llama3.1 8b					
	0	0.44	57.88	[0.43, 0.46]	< .001 ***
	1	0.31	47.93	[0.30, 0.32]	< .001 ***
	2	0.35	50.93	[0.34, 0.36]	< .001 ***
	3	0.33	44.14	[0.32, 0.35]	< .001 ***
	5	0.34	47.85	[0.33, 0.36]	< .001 ***
	8	0.33	36.62	[0.32, 0.35]	< .001 ***
gemma3 12b					
	0	0.38	47.04	[0.36, 0.40]	< .001 ***
	1	0.32	32.91	[0.30, 0.34]	< .001 ***
	2	0.31	35.37	[0.29, 0.32]	< .001 ***
	3	0.33	32.26	[0.31, 0.35]	< .001 ***
	5	0.32	33.27	[0.30, 0.34]	< .001 ***
	8	0.30	30.84	[0.28, 0.32]	< .001 ***
gemma3 27b					
	0	0.33	41.39	[0.31, 0.34]	< .001 ***
	1	0.34	36.93	[0.32, 0.36]	< .001 ***
	2	0.35	44.59	[0.33, 0.36]	< .001 ***
	3	0.33	37.60	[0.31, 0.35]	< .001 ***
	5	0.36	38.50	[0.34, 0.38]	< .001 ***
	8	0.37	43.22	[0.36, 0.39]	< .001 ***
mistral3.2 24b					
	0	0.37	46.34	[0.35, 0.39]	< .001 ***
	1	0.33	44.02	[0.32, 0.35]	< .001 ***
	2	0.33	45.06	[0.32, 0.34]	< .001 ***
	3	0.33	43.10	[0.32, 0.35]	< .001 ***
	5	0.34	49.22	[0.32, 0.35]	< .001 ***
	8	0.35	52.00	[0.34, 0.36]	< .001 ***

Note: *Second-level t-test results reflect estimated mean Pearson correlations from first-level RSA.*

Table S5

"Best-fitting" Katz γ from the next-node prediction task.

LLM	# steps	Mean γ	Median γ
llama3.1 8b			
	0	0.423	0.40
	1	0.444	0.40
	2	0.269	0.10
	3	0.367	0.30
	5	0.418	0.40
	8	0.426	0.40
gemma3 12b			
	0	0.335	0.25
	1	0.381	0.30
	2	0.394	0.30
	3	0.384	0.30
	5	0.405	0.30
	8	0.486	0.45
gemma3 27b			
	0	0.301	0.10
	1	0.314	0.10
	2	0.346	0.20
	3	0.393	0.40
	5	0.401	0.30
	8	0.398	0.40
mistral3.2 24b			
	0	0.227	0.10
	1	0.347	0.20
	2	0.252	0.10
	3	0.331	0.10
	5	0.321	0.20
	8	0.249	0.10